Deuterated Δ^7-Cholestenol Analogues as Mechanistic Probes for Wild-Type and Mutated Δ^7-Sterol-C5(6)-desaturase

Alain Rahier*

Département Isoprénoïdes, Institut de Biologie Moléculaire des Plantes, CNRS FRE 2161, 28 rue Goethe, 67083 Strasbourg Cédex, France

Received July 21, 2000; Revised Manuscript Received October 4, 2000

ABSTRACT: Deuterium-labeled 5α-cholest-7-en-3β-ol (**1**) bearing one or two deuteriums at the C-5α and (or) C-6α positions was synthesized in high isotopic and chiral purity. These compounds were used as substrates with the microsomal wild-type *Zea mays* and recombinant *Arabidopsis thaliana* Δ^7-sterol-C5-(6)-desaturases (5-DES) to probe directly the stereochemistry and the mechanism of the enzymatic reaction. Clearly, in the conversion of **1** by both 5-DESs, the 6α-hydrogen is removed. [6α-^{2}H]-5α-Cholest-7-en-3β-ol shows an intermolecular deuterium kinetic isotope effect (DKIE) on *V* and *V*/*K*, $^{D6}V = 2.6 \pm 0.3$, $^{D6}V/K = 2.4 \pm 0.1$; and $^{D6}V = 2.3 \pm 0.3$, $^{D6}V/K = 2.3 \pm 0.2$ for the *Zea mays* and *A. thaliana* wild-type 5-DES, respectively. In contrast, negligible or minor isotope effects, $^{D5}V = 0.99 \pm 0.04$, $^{D5}V/K = 0.91 \pm 0.08$; and $^{D5}V = 0.93 \pm 0.06$, $^{D5}V/K = 0.96 \pm 0.04$, respectively, were observed with [5α-^{2}H]-cholest-7-en-3β-ol. The observed pattern of isotope effects strongly suggests that the plant 5-DES initiates oxidation by cleavage of the chemically activated C6α−H bond, a step which appears to be partially rate-limiting in the desaturation process. Cleavage of the C5−H bond has a negligible isotope effect, indicating that the desaturation involves asynchronous scission of the two C−H bonds at C5 and C6. We showed previously [Taton, M., et al. (2000) *Biochemistry 39,* 701] that threonine 114 was not essential to maintaining desaturase activity, although *V*/*K* values for mutant T114I and T114S were respectively 10-fold lower and 4-fold higher than that of the native 5-DES. In this study, we combined variation in enzyme structure and DKIE studies and showed that ^{D6}V and $^{D6}V/K$ increased respectively to 3.8 ± 0.3 and 3.8 ± 0.4 in mutant T114I and decreased respectively to 1.6 ± 0.4 and 1.7 ± 0.1 in mutant T114S. The data suggest that the conserved hydroxyl function at position 114 in the ERG3 family makes the abstraction of the 6α-hydrogen atom substantially less rate-limiting during the 5-DES reaction. Based on the data, a tentative mechanism for the desaturation of cholest-7-en-3β-ol is proposed.

During sterol biosynthesis in plants and animals, the 9β,-19-cyclopropyl ring- or Δ^8-unsaturation of cycloartenol and lanosterol, respectively, is transposed via a multienzymatic cascade to the double bond at the C5(6) position (*1*, *2*). We have recently shown that in higher plants (*3*), Δ^7-sterol-C5-(6)-desaturase (EC 1.3.3.2) (5-DES)[1] also processes the desaturation of Δ^7-sterol precursors to produce $\Delta^{5,7}$-sterols as in mammals (*4*) and yeast (*5*) (Figure 1). 5-DES is membrane-bound, requires molecular oxygen, is strongly promoted by NAD(P)H, is inhibited by cyanide, hydrophobic chelators, and cytochrome *c*, and is insensitive to carbon monoxide. In addition, membrane-bound cytochrome b_5 is an obligate carrier of electrons from NAD(P)H via NADH cyt b_5 reductase to the mammalian (*6*) and plant (*7*) 5-DESs. The cDNA or genes encoding 5-DES have been characterized in a variety of organisms including *Saccharomyces cerevisiae* (*8*), *Arabidopsis thaliana* (*9*), *Homo sapiens* (*10*), and *Candida glabrata* (GenBank L40390). These proteins differ slightly in size, and the *A. thaliana* 5-DES shares only 29%, 35%, and 29% identity with the yeast, human, and *Candida* 5-DES, respectively. Moreover, the 5-DESs possess a central portion containing well-conserved residues, including three conserved histidine-rich motifs which are found in an important class of integral membrane enzymes that includes desaturases, hydroxylases, epoxidases, and acetylenases (*11*−*14*). In one of these enzymes, rat stearoyl-CoA desaturase, eight histidine residues from three histidine-rich motifs were shown to be essential for catalysis (*11*). Recently we have demonstrated that the *A. thaliana* 5-DES can be functionally active when expressed in the yeast *erg 3* null mutant, and we showed by mutational analysis coupled with kinetic studies that the eight histidine residues from the three histidine-rich motifs of the 5-DES were essential for catalysis (*15*). One possible function for these motifs would be to

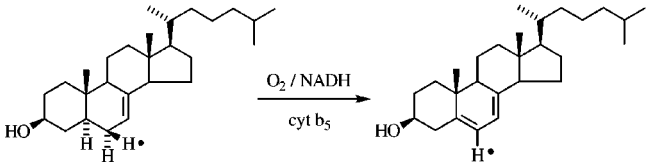

FIGURE 1: Reaction catalyzed by Δ^7-sterol-C5(6)-desaturase.

* Phone: 0033388358362. Fax: 0033388358484. E-mail: enzymo@bota-ulp.u-strasbg.fr.

[1] Abbreviations: 5-DES, Δ^7-sterol-C5(6)-desaturase; cyt b_5, cytochrome b_5; GC-MS, coupled gas chromatography−mass spectroscopy; HPLC, high-pressure liquid chromatography; P450, cytochrome P450; TLC, thin-layer chromatography; GC, gas chromatography; EI, electron impact.

10.1021/bi001696b CCC: $20.00
Published on Web 12/09/2000

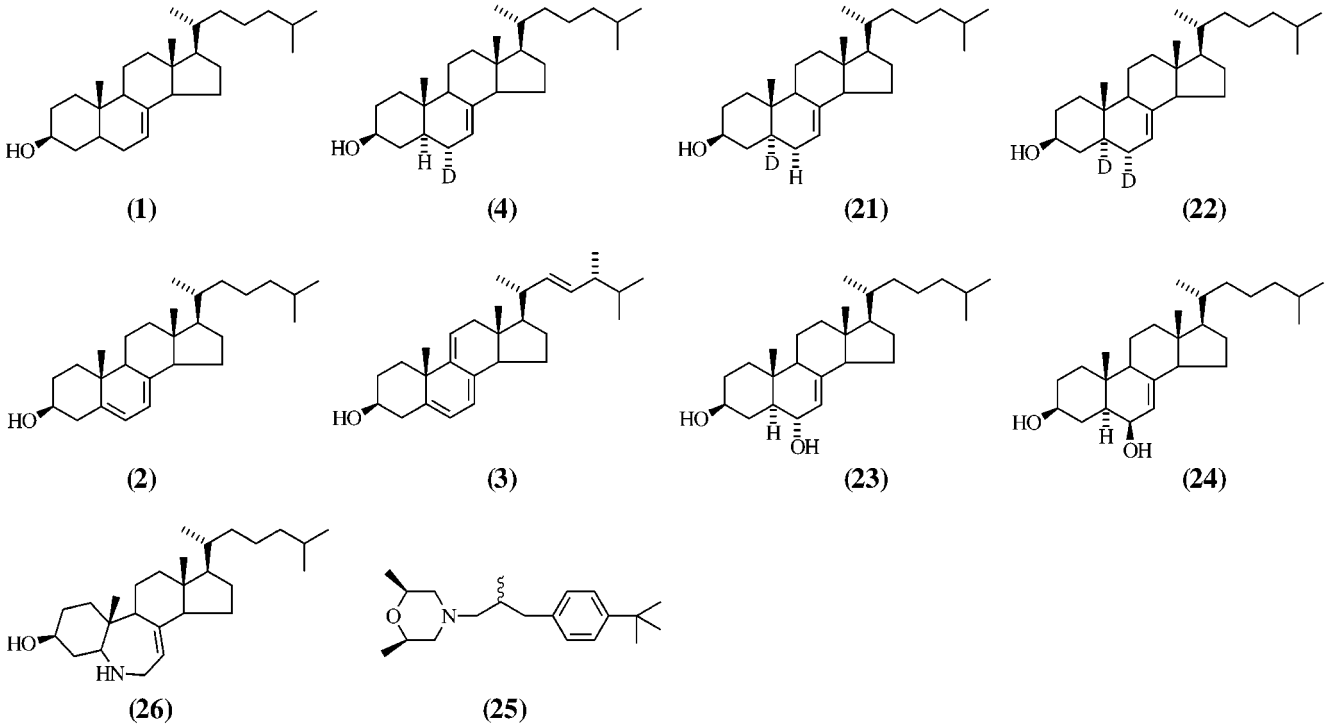

FIGURE 2: Chemical structures of the compounds used in the present study.

provide the ligands for a presumed catalytic Fe center, as previously proposed for this class of integral membrane enzymes catalyzing desaturations and hydroxylations (*11*). Indeed, spectroscopic studies of alkane ω-hydroxylase provided evidence that a diiron cluster is present in at least one member of this class of integral membrane enzymes (*13*). In contrast, a second type of desaturases, which correspond to the soluble plant enzymes and use the acyl carrier protein of the substrate fatty acid, have a consensus motif consisting of carboxylates and histidines that are thought to coordinate an active diiron cluster (*16*).

In the ERG3 family, 5-DESs from different organisms possess a conserved hydroxyl function at position 114 (*15*). We recently found that threonine 114 was not essential to maintaining the *A. thaliana* 5-DES activity (*15*). However, *V*/*K* values for mutants T114I and T114S were respectively 10-fold lower and 4-fold higher than that of the native 5-DES, suggesting that a hydroxyl-containing side chain at position 114 substantially increases the catalytical rate of the *A. thaliana* 5-DES (*15*).

Very little work on the detailed mechanism of membrane-bound fatty acid and steroid desaturating enzymes has appeared over the past 3 decades, and the mechanism by which the 5-DES catalyzes the desaturation of Δ^7-sterols remains unknown. Moreover, while considerable experimental detail is available on the catalytic mechanism and the role of residues affecting the activity of P450 monooxygenases, less is known about the mode of action of the small family of non-heme iron membrane-bound hydroxylases and desaturases to which the 5-DES most probably belongs. This is primarily due to the difficulty of obtaining an in vitro functional enzymatic system able to carry out lipid desaturation reactions, since, to our knowledge, all the reported mechanistic studies on desaturases described so far are based on the in vivo metabolism of labeled substrates or precursors.

To get insights into the catalytic mechanism of the 5-DES, we measured directly in vitro, in a microsomal preparation containing the 5-DES, the effects of deuterium substitution at C5 and C6 on the kinetic constants of the desaturase. We report first the synthesis and characterization of [5α]-, [6α]-, and [5α, 6α]-deuterated forms of 5α-cholest-7-en-3β-ol (**1**) (Figure 2). Second, we describe their use to (i) probe the stereochemistry of the reaction and (ii) determine the intermolecular primary deuterium kinetic isotope effect (DKIE) on the kinetic constants V_{max} and V_{max}/K_m for the removal of the 5α- and 6α-hydrogens of **1** catalyzed either by the wild-type *Zea mays* or by the recombinant *Arabidopsis thaliana* Δ^7-sterol-C5(6) desaturase. Third, we combine this methodology with variation of enzyme structure to find information on the role that the previously identified key residue, Thr114, exerts on catalysis carried out by the *A. thaliana* 5-DES.

MATERIALS AND METHODS

Chemical and Reagents. The following chemicals and reagents were purchased from Sigma: β-NADH (disodium salt), NAD^+, glutathione (reduced form), Trizma base, 5α-cholest-7-en-3β-ol (**1**), and ergosta-5,7,9,22-tetraen-3β-ol (**2**).

Silica gel (230−400 mesh) was used for flash chromatography. Analytical and semipreparative TLC were performed using Merck glass plates precoated with silica G/UV254. Unless otherwise stated, all reagents were purchased from Aldrich Chemical Co. and used without purification.

Chemical Procedures. Melting points are uncorrected. MS and GC-MS were determined at 70 eV with a MD800 Fison spectrometer. The GC separation was carried out on a capillary column (WCOT; 30 m length × 0.25 mm inner diameter) coated with DB1 (J & W Scientific, Folston, CA). The deuterium content was estimated from the average of MS scans across the GC peak and has been corrected for

Scheme 1[a]

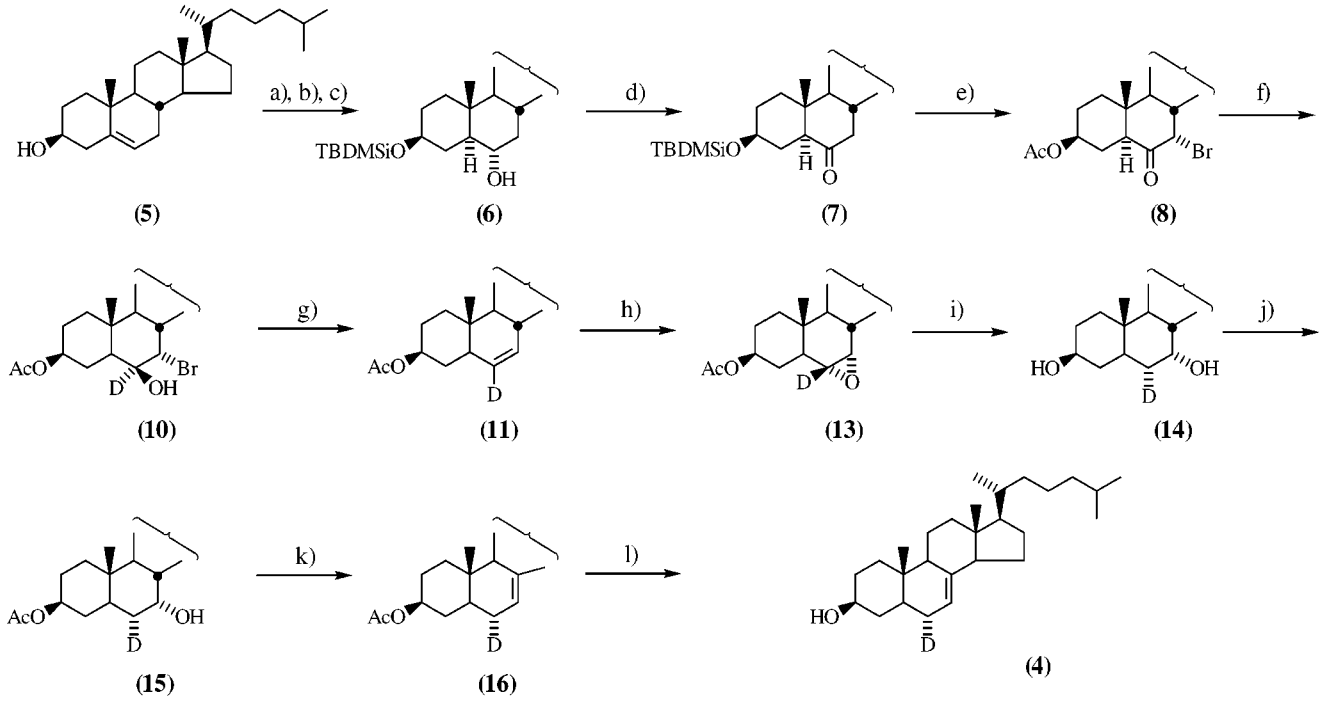

[a] a), TBDMS-Cl, imidazole; b) BH_3−THF; c) ^-OH, H_2O_2; d) Cr_2O_7−pyridine, CH_2Cl_2; e) Br_2, AcOH, Et_2O; f) $NaBD_4$, THF/MeOD; g) Zn, AcOH; h) MCPA, CH_2Cl_2; i) $LiAlH_4$, Et_2O; j) Ac_2O, pyridine; k) $POCl_3$, pyridine; l) KOH, MeOH.

natural isotopic abundances. GC analyses were carried out with a GC instrument (model 8300, Varian, Les Ulis, France) equipped with a flame ionization detector and a fused capillary column (WCOT; 30 m length × 0.25 mm inner diameter) coated with DB1 (H_2 flow, 2 mL/min). The temperature used included a 30 °C/min rise from 60 to 240 °C and then a 2 °C/min rise from 240 to 280 °C. Relative retention times (t_R) are given with respect to cholesterol (t_R = 1). HPLC analysis was carried out with a Waters S10 instrument equipped with a single pump and linked to an ultraviolet spectrophotometric detector. Separations were carried out with two analytical C18 ultrasphere 5 μm columns (250 × 4.6 mm) in line, from Beckman, with a flow rate of 1 mL/min at room temperature. Proton magnetic resonance was monitored in a [^{2}H]chloroform solution at 400 MHz with a Bruker spectrometer. Chemical shifts (δ) in parts per million were determined relative to tetramethylsilane. *J* values are in hertz.

*Synthesis of [6α-^{2}H]-5α-Cholest-7-en-3β-ol (**4**) (Figure 2).* This substrate was prepared as shown in Scheme 1. Part of the synthesis was performed according to modifications of the procedure of Akhtar and Marsh (*17*), used for the synthesis of [6α-tritiated]-5α-cholest-7-en-3β-ol.

*6α-Hydroxy-5α-cholestan-3β-tert-butyldimethylsilyl Ether (**6**).* The 3β-hydroxyl function of cholesterol (**5**) (7.7 g) was silylated according to standard procedure (*18*), yielding 5α-cholestan-3β-*tert*-butyldimethylsilyl ether (9.7 g) which was subsequently dissolved in dry tetrahydrofuran (150 mL) under an atmosphere of argon and treated by a 1 M solution of borane in tetrahydrofuran (200 mL) at 0 °C. The reaction mixture was allowed to react at room temperature overnight. The reaction mixture was then treated with a solution of 5% NaOH in water (200 mL) and 30% H_2O_2 (70 mL) and allowed to react for 5 h at room temperature. The reaction mixture was then diluted with water and extracted with hexane. The organic layer was washed with a solution of ferrous sulfate ($FeSO_4$) in water, dried over $MgSO_4$, filtered, evaporated, and dried under vacuum. The resulting residue was crystallized from MeOH/CH_2Cl_2 to yield pure **6** (6.5 g) as determined from the 400 MHz ^{1}H NMR spectrum: mp 146−148 °C; MS (EI) *m*/*e* (relative intensity) M^+ = 518-(0.5), 461(12), 443(4), 385(4), 369(90); ^{1}H NMR (400 MHz, $CDCl_3$) δ 0.054 (6H, s, Me-Si), 0.645 (3H, s, H18), 0.806 (3H, s, H19), 0.860 (3H, d, *J* = 6.6, H26 or -27), 0.864 (3H, d, *J* = 6.6, H26 or -27), 0.884 (9H, s, tBu), 0.899 (3H, d, *J* = 6.5, H21), 3.399 (1H, m, H3α), 3.513 (1H, ddd, *J* = 14.3, 4.9, 4.9, H6β).

*5α-Cholestan-6-one-3β-tert-butyldimethylsilyl Ether (**7**).* **6** (6 g) in anhydrous methylene chloride (CH_2Cl_2) (150 mL) was stirred with pyridium dichromate (10 g) for 2 days at 20 °C under an atmosphere of argon according to Corey and Schmidt (*19*). Filtration of the reaction mixture over $MgSO_4$ and evaporation of the organic layer to dryness afforded a residue which was recrystallized from MeOH/CH_2Cl_2 to yield pure **7** (5 g): mp 172−174 °C; MS (EI) *m*/*e* (relative intensity) M^+-tBu = 459(100), 367(4); ^{1}H NMR (400 MHz, $CDCl_3$) δ 0.039 (6H, s, MeSi), 0.656 (3H, s, H18), 0.748 (3H, s, H19), 0.865 (3H, d, *J* = 7, H26 or -27), 0.867 (3H, d, *J* = 7, H26 or -27), 0.873 (9H, s, tBu), 0.912 (3H, d, *J* = 6.5, H21), 2.033 (1H, ddd, *J* = 12.7, 2.7, 2.7, H7β), 2.165 (1H, dd, *J* = 12.7, 2.4 H7α), 2.311 (1H, dd, *J* = 13, 4.4, H5α), 3.519 (1H, m, H3α).

*7α-Bromo-5α-cholestan-6-on-3β-yl Acetate (**8**).* To a solution of **7** (3.8 g) in dry diethyl ether (Et_2O) (100 mL) and acetic acid (13 mL) was added dropwise bromine (380 μL) in acetic acid (15 mL). The resulting solution was refluxed for 22 h at 40 °C under an atmosphere of argon. The ether layer was then added to water and the mixture extracted with hexane. The organic layer was washed with a 10% solution of $NaHCO_3$ in water, dried over $MgSO_4$,

and concentrated to dryness. The residue was purified by flash chromatography on silica gel eluting with CH_2Cl_2, yielding a fraction (2.4 g) containing a 1/1 mixture of 7α-bromo-5α-cholestan-6-on-3β-yl acetate (**8**) and 5α-bromo-cholestan-6-on-3β-yl acetate (**9**) as determined by ^{1}H NMR spectra at 400 MHz: MS (EI) *m*/*e* (relative intensity) M^+ = 522/524(3/3), 462/464(24/24), 443(8), 383(100), 382(40), 243(17), 229(35); ^{1}H NMR (400 MHz, $CDCl_3$) (**8**): δ 0.689 (3H, s, H18), 0.863 (3H, d, J = 7, H26 or -27), 0.867 (3H, d, J = 7, H26 or -27), 0.921 (3H, d, J = 6.5, H21), 0.985 (3H, s, H19), 2.033 (3H, s, acetate), 3.286 (1H, dd, J = 12.4, 2.9, H5α), 4.183 (1H, d, J = 3.5, H7β), 4.728 (1H, m, H3α).

*[6-^{2}H]-5α-Cholest-6-en-3β-yl Acetate (**11**).* To the above mixture of **8** and **9** (2.2 g) in a 1/1 mixture of dry tetrahydrofuran and deuterated methanol (THF/MeOD) (120 mL) at 0 °C was added an excess of sodium deuteriobo-rohydride ($NaBD_4$), and the mixture was stirred for 16 h at 4 °C after which no more starting material was detected by TLC. The excess hydride was decomposed by the addition of diluted H_2SO_4 and the reaction mixture extracted with hexane. The organic layer was dried over $MgSO_4$, filtered, and concentrated to dryness. Control TLC indicated the formation of three major products. The dry residue (2 g) was then dissolved in glacial acetic acid (150 mL), and the resulting solution was vigorously stirred and refluxed with Zn powder (6 g) at 120 °C for 15 min under an atmosphere of argon. The suspension was filtered on $MgSO_4$ and washed with hexane. The acetic solution was extracted with hexane with addition of water to obtain two phases. The hexane layer was washed with a $NaHCO_3$ solution and water, dried over $MgSO_4$, and concentrated to dryness. The residue (1.6 g) was crystallized from MeOH/CH_2Cl_2 to yield **11** (1.0 g) with 90% purity as determined by 400 MHz ^{1}H NMR spectra. **11**: mp 95−97 °C; MS (EI) *m*/*e* (relative intensity) M^+ = 429(27), 428(0), 414(7), 369(100), 354(32), 256(57), 230-(13), 214(31). The product was 100% monodeuterated. ^{1}H NMR (400 MHz, $CDCl_3$): δ 0.689 (3H, s, H18), 0.794 (3H, s, H19), 0.861 (3H, d, J = 6.6, H26 or -27), 0.865 (3H, d, J = 6.6, H26 or -27), 0.907 (3H, d, J = 6.5, H21), 2.030 (3H, s, acetate), 4.735 (1H, m, H3α), 5.477 (1H, s, ω1/2 = 5, H7). The small contaminant was identified as [6-^{2}H]-cholest-5-en-3β-yl acetate. The similar sequence of reactions was performed using $NaBH_4$ instead of $NaBD_4$. This sequence afforded 5α-cholest-6-en-3β-acetate (**12**) with 90% purity, allowing the ^{1}H NMR signals of the C6 and C7 vinylic protons to be unambiguously assigned. **12**: ^{1}H NMR (400 MHz, $CDCl_3$) δ 0.689 (3H, s, H18), 0.795 (3H, s, H19), 0.861 (3H, d, J = 6.6, H26 or -27), 0.865 (3H, d, J = 6.6, H26 or H27), 0.907 (3H, d, J = 6.5, H21), 2.031 (3H, s, acetate), 4.735 (1H, m, H3α), 5.242 (1H, d, J = 9.9, H6), 5.479 (1H, d, J = 9.9, H7).

*6α,7α-Epoxy-[6β-^{2}H]-5α-cholestan-3β-yl Acetate (**13**).* To a stirred solution of *m*-chloroperbenzoic acid (600 mg) in CH_2Cl_2 (30 mL) at 0 °C was added compound **11** (950 mg) dissolved in CH_2Cl_2 (20 mL) at 0 °C, and the mixture was reacted for 16 h at 4 °C under an atmosphere of argon. After usual workup, the dry residue was crystallized from MeOH, affording pure **13** (450 mg): mp 171−173 °C [Akhtar and Marsh, 1967 (*17*), quote 175 °C]. The product had >98% purity as determined by integration of the 400 MHz ^{1}H NMR signals. MS (EI) *m*/*e* (relative intensity): M^+ = 445(24), 430-(2), 427(2), 412(2), 385(100), 370(10), 367(11), 352(8), 314-(5), 230(16), 212(10). The measured deuteration rate on the molecular ion was 1% d_0, 99% d_1. ^{1}H NMR (400 MHz, $CDCl_3$): δ 0.704 (3H, s, H18), 0.791 (3H, s, H19), 0.861 (3H, d, J = 6.6, H26 or -27), 0.866 (3H, d, J = 6.6, H26 or -27), 0.903 (3H, d, J = 6.6, H21), 2.038 (3H, s, acetate), 3.030 (1H, d, J = 2.3, H7β), 4.740 (1H, m, H3α). The β-equatorial stereochemistry of the single epoxide proton at C7 of **13** was determined from its ^{1}H NMR spectrum since this proton appeared as a doublet with a small 1,2 equatorial−axial coupling constant (J = 2.3 Hz).

*[6α-^{2}H]-5α-Cholestane-3β,7α-diol (**14**).* An excess of $LiAlH_4$ was added slowly to **13** (350 mg) dissolved in anhydrous Et_2O (20 mL) under an atmosphere of argon. The reaction mixture was stirred and refluxed for 24 h and then worked up in the usual way, affording a residue which was purified by TLC on silica gel G eluting with CH_2Cl_2/MeOH (98/2, v/v, two developments). The major fraction afforded **14** (225 mg) with a purity >98% as determined by the 400 MHz ^{1}H NMR spectrum and GC analysis. The same reaction carried out on the crystallization mother liquor of **13** afforded additional pure **14** (85 mg) after TLC purification. **14**: mp 152−154 °C [Akhtar and Marsh (*17*) quote mp 148 °C, Fieser and Heymann (*20*) quote mp 152 °C]. MS (EI) *m*/*e* (relative intensity): M^+ = 405(24), 387(100), 372(22), 369-(6), 354(7), 274(13), 250(69), 232(15), 214(23). The compound was 100% monodeuterated. ^{1}H NMR (400 MHz, $CDCl_3$) δ: 0.659 (3H, s, H18), 0.807 (3H, s, H19), 0.860 (3H, d, J = 6.6, H26 or H27), 0.864 (3H, d, J = 6.6, H26 or H27), 0.907 (3H, d, J = 6.6, H21), 3.631 (1H, m, H3α), 3.830 (1H, broad s, ω1/2 = 7.4, H7β). The absence of a large 1,2 axial−axial coupling constant in the signal of the proton at C7 was consistent with the assigned 7α-axial stereochemistry for the hydroxyl at C7.

*[6α-^{2}H]-5α-Cholestan-7α-ol-3β-yl Acetate (**15**).* To **14** (200 mg) dissolved in anhydrous pyridine (1 mL) was added acetic anhydride (37 μL), and the reaction mixture was kept for 16 h at 20 °C under an atmosphere of argon. Usual workup afforded a residue which was purified by TLC on silica gel G eluting with CH_2Cl_2/MeOH (98/2, v/v). The major band afforded **15** (142 mg) with a purity >98% as determined by GC analysis and 400 MHz ^{1}H NMR spectroscopy (**15**): mp 112−114 °C from MeOH/CH_2Cl_2; MS (EI) *m*/*e* (relative intensity) M^+ = 447(25), 429(100), 414-(17), 387(14), 369(67), 354(13), 292(67), 256(17), 214(37). The deuteration rate was 2% d_0, 98% d_1. ^{1}H NMR (400 MHz, $CDCl_3$) δ: 0.656 (3H, s, H18), 0.821 (3H, s, H19), 0.859 (3H, d, J = 6.6, H26 or -27), 0.864 (3H, d, J = 6.6, H26 or -27), 0.906 (3H, d, J = 6.5, H21), 2.014 (3H, s, acetate), 3.820 (1H, broad s, ω1/2 = 7.5, H7β), 4.710 (1H, m, H3α).

*[6α-^{2}H]-5α-Cholest-7-en-3β-yl Acetate (**16**).* To compound **15** (120 mg) in anhydrous pyridine (2 mL) was added freshly distilled phosphorus oxychloride $POCl_3$ (2 mL). The reaction was refluxed for 1 h under an atmosphere of argon. It was cooled and extracted with Et_2O. The organic layer was washed with ice/water, $NaHCO_3$ solution, and again with water, dried over $MgSO_4$, filtered, and evaporated to dryness. The residue was purified by TLC on silica gel G impregnated with 10% $AgNO_3$ (solvent: cyclohexane/toluene, 7/3, v/v). The fraction migrating as an authentic standard of 5α-cholest-7-en-3β-yl acetate was collected and recrystallized from MeOH, affording **16** (42 mg) with a purity >98% as determined by GC analysis and 400 MHz ^{1}H NMR spec-

Scheme 2[a]

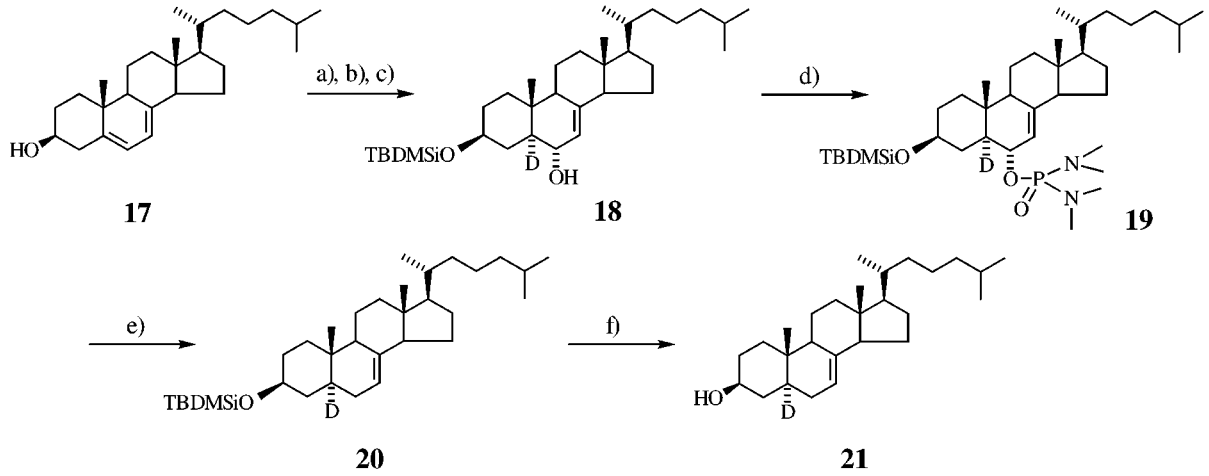

[a] a) TBDMS-Cl, imidazole; b) BD_3−THF; c) ^-OH, H_2O_2; d) nBuLi, $ClP(O)(NMe_2)_2$; e) Li, $EtNH_2$, tBuOH; f) $N(Bu)_4F$.

troscopy. **16**: mp 112−114 °C; MS (EI) *m*/*e* (relative intensity) $M^+ = 429(83)$, 414(16), 369(3), 354(8), 256(100), 214(43). The deuteration rate was 2% d_0, 98% d_1. ^1H NMR (400 MHz, $CDCl_3$) δ: 0.532 (3H, s, H18), 0.863 (3H, d, J = 6.6, H26 or -27), 0.867 (3H, d, J = 6.6, H26 or -27), 0.919 (3H, d, J = 6.5, H21), 2.014 (3H, s, acetate), 4.694 (1H, m, H3α), 5.142 (1H, d, J = 1.8 Hz, H7).

*[6α-^{2}H]-5α-Cholest-7-en-3β-ol (**4**).* Compound **16** (34 mg) was saponified with 6% KOH in MeOH, yielding **4** which was crystallized from MeOH. **4** (24 mg): mp 123−125 °C; MS (EI) *m*/*e* (relative intensity) $M^+ = 387(100)$, 372(36), 354(10), 274(26), 256(91), 230(27). **4** was 100% monodeuterated based on the MS data. ^1H NMR (400 MHz, $CDCl_3$) δ: 0.534 (3H, s, H18), 0.796 (3H, s, H19), 0.863 (3H, d, J = 6.6, H26 or -27), 0.867 (3H, d, J = 6.6, H26 or -27), 0.919 (3H, d, J = 6.5, H21), 3.593 (1H, m, H3α), 5.154 (1H, d, J = 1.7, H7).

*Synthesis of [5α-^{2}H]-Cholest-7-en-3β-ol (**21**)*

*[5α-^{2}H]-6α-Hydroxycholest-7-en-3β-tert-butyldimethylsilyl Ether (**18**) (Scheme 2).* The 3β-hydroxyl function of cholesta-5,7-dien-3β-ol (**17**) was silylated according to standard procedure (*18*), yielding cholesta-5,7-dien-3β-*tert*-butyldimethylsilyl ether.

To a solution of $NaBD_4$ (400 mg) in dry THF (40 mL) at 0 °C under an atmosphere of argon was added dropwise boron trifluoride−etherate complex (BF_3−Et_2O) (931 mg, 824 μL), and the mixture was reacted for 30 min at 0 °C. Cholesta-5,7-dien-3β-*tert*-butyldimethylsilyl ether (1.8 g) in dry THF (10 mL) was then added, and the reaction mixture was stirred for 16 h at 4 °C and then for 3 h at 20 °C. The reaction was then treated with a solution of 5% NaOH (60 mL) and 30% H_2O_2 (30 mL) and allowed to react for 3 h at room temperature. The reaction mixture was worked up as above for the synthesis of **6**. Control TLC of the residue indicated the formation of one major product (>80%). The residue was then crystallized twice from MeOH/CH_2Cl_2 to afford pure **18** (1.1 g) as determined by GC analysis and 400 MHz ^1H NMR spectroscopy. **18**: mp 165−167 °C; MS (EI) *m*/*e* (relative intensity) $M^+ = 517(4)$, 499(31), 498(13), 484(5), 460(20), 442(22), 441(6), 386(22), 384(33), 368(100), 366(38), 254(75), 253(32). The deuteration rate measured on peak 460 was 5% d_0, 95% d_1. ^1H NMR (400 MHz, $CDCl_3$) δ: 0.061 (3H, s, MeSi), 0.540 (3H, s, H18), 0.834 (3H, s, H19), 0.864 (3H, d, J = 6.6, H26 or -27), 0.869 (3H, d, J = 6.6, H26 or -27), 0.889 (9H, s, tBu), 0.919 (3H, d, J = 6.5, H21), 3.539 (1H, m, H3α), 3.794 (1H, broad s, ω1/2 = 12, H6β), 5.177 (1H, d, J = 1.9, H7). The ^1H NMR spectrum of **18** was in full accordance with that described for the corresponding 3,3-(ethylenedioxy)-5α-cholest-7-en-6α-ol by Dolle et al. (*21*). Particularly δ = 0.83 ppm (CH_3-19) attested an A/B trans ring junction, i.e., 5α-^{2}H, involving an equatorial and stable 6α-hydroxyl group through the well-known cis-addition of boranes (δ CH_3-19A/B cis = 1.07 ppm).

*[5α-^{2}H]-Cholest-7-en-3β-tert-butyldimethylsilyl Ether (**20**).* Compound **18** (1 g) was dissolved in a mixture of anhydrous THF (40 mL) and anhydrous triethylamine (Et_3N) (10 mL) under an atmosphere of argon. The mixture was treated with *n*-butyllithium in solution in hexane (1.6 M, 2.5 mL) and reacted 5 min at 25 °C. Then *N*,*N*,*N*′,*N*′-tetramethyldiamidophosphorochloridate (1.6 mL) was added, and the mixture was reacted for 3 h at 25 °C. The reaction was stopped by addition of water and extracted with diethyl ether. The organic layer was washed with water, dried with $MgSO_4$, and evaporated to dryness. Control TLC indicated the absence of any starting **18**. The residue was dried under vacuum and dissolved in dry THF (20 mL) at −20 °C. Dry ethylamine ($EtNH_2$) (80 mL) at −20 °C and lithium (140 mg) were then added, and the mixture was stirred for 20 min at −20 °C. To the blue solution was added 200 μL of dry tertiobutanol, and the mixture was reacted for an additional 20 min at −20 °C under argon. The blue solution was then made colorless by addition of NH_4Cl, and $EtNH_3$ was evaporated. Water was added, and the mixture was extracted with hexane. The organic layer was washed with water, dried over $MgSO_4$, and evaporated to dryness. The residue was crystallized from MeOH/CH_2Cl_2 to afford **20** (800 mg) with >98% purity as determined by (i) GC analysis, (ii) ^1H NMR spectroscopy, and (iii) $AgNO_3$/SiO_2 TLC using cyclohexane/toluene (9/1, v/v) as eluting solvent. **20**: mp 146−148 °C; MS (EI) *m*/*e* (relative intensity) $M^+ = 501(1)$, 486(2), 444(100), 369(13). The deuteration rate was 100% d_1 on ion 444. ^1H NMR (400 MHz, $CDCl_3$) δ: 0.050 (6H, s, Si-Me), 0.527 (3H, s, H18), 0.862 (3H, d, J = 6.6, H26 or -27), 0.867 (3H, d, J = 6.6, H26 or -27), 0.885 (9H, s, tBu), 0.917 (3H, d, J = 6.5, H21), 3.545 (1H, m, H3α), 5.151 (1H, broad s, ω1/2 = 9 Hz, H7).

*[5α-^{2}H]-Cholest-7-en-3β-ol (**21**).* **20** (150 mg) was deprotected by treatment with tetrabutylammonium fluoride adsorbed on SiO_2, for 16 h at 20 °C in THF (8 mL). Usual workup yielded pure **21** which was crystallized from MeOH. **21** (80 mg): mp 120−122 °C; MS (EI) *m*/*e* (relative intensity) M^+ = 387(100), 372(36), 354(8), 274(21), 256(85), 230(23). The deuteration rate was 2% d_0, 98% d_1. ^{1}H NMR (400 MHz, $CDCl_3$) δ: 0.534 (3H, s, H18), 0.795 (3H, s, H19), 0.862 (3H, d, J = 6.6, H26 or -27), 0.867 (3H, d, J = 6.6, H26 or -27), 0.919 (3H, d, J = 6.5, H21), 3.592 (3H, m, H3α), 5.157 (1H, dd, J = 4.8, J = 2.3, H7).

*Synthesis of [5α-^{2}H, 6α-^{2}H]-Cholest-7-en-3β-ol (**22**).* This substrate was prepared according to modifications of the procedure of Paliokas and Schroepfer (*22*) as described below. To cholesta-5,7-dien-3β-ol (300 mg) dissolved in dry THF (80 mL) were added cupric acetate [$Cu(SO_4)_2$ (1.6 mg)], deuterated hydrazine hydrate (40 mL of a 25% w/v solution in D_2O), and MeOD (20 mL) as to obtain a single phase. The mixture was reacted while stirring for 2 days at 20 °C, after which the composition of the reaction mixture did not change on control TLC's. The mixture was then extracted with hexane, and the organic layer was dried over $MgSO_4$ and evaporated to dryness to afford a solid residue, which was purified by TLC on 10% $AgNO_3$-impregnated alumina (Al_2O_3) using chloroform/hexane/acetone (6/3/1, v/v/v) as the developing solvent. The fraction migrating like an authentic standard of 5α-cholest-7-en-3β-ol was eluted from the alumina and crystallized from MeOH to yield pure **22** (28 mg) as determined by GC analysis and 400 MHz ^{1}H NMR spectroscopy. **22**: mp 120−122 °C; MS (EI) *m*/*e* (relative intensity) M^+ = 388(100), 373(38), 355(5), 275(19), 257(64), 233(20), 215(18). The deuteration rate calculated on the molecular peak M^+ was 0% d_0, 3% d_1, 97% d_2, 0% d_3, indicating more than 98% deuteration on each of the 5α and 6α positions. ^{1}H NMR (400 MHz, $CDCl_3$) δ: 0.535 (3H, s, H18), 0.796 (3H, s, H19), 0.863 (3H, d, J = 6.6, H26 or -27), 0.867 (3H, d, J = 6.6, H26 or -27), 0.921 (3H, d, J = 6.5, H21), 3.592 (1H, m, H3α), 5.154 (1H, d, J = 1.9 Hz, H7).

*Synthesis of 5α-Cholest-7-en-3β,6α-diol (**23**) and 5α-Cholest-7-en-3β,6β-diol (**24**)*

*5α-Cholest-7-en-3β,6α-diol (**23**).* 6α-Hydroxy-5α-cholestan-7-en-3β-*tert*-butyldimethylsilyl ether (25 mg), prepared from **17** as described for the synthesis of **18**, was deprotected by stirring with tetrabutylammonium fluoride adsorbed on SiO_2, for 24 h at 20 °C in THF (5 mL) under an atmosphere of argon. Usual workup and recrystallization from MeOH yielded pure **23** (10 mg): mp 191−193 °C [Dolle et al. (*21*) quote 192 °C]; MS (EI) *m*/*e* (relative intensity) M^+ = 402(100), 384(68), 369(28), 366(11), 351(90), 271(67), 253(48); ^{1}H NMR (400 MHz, $CDCl_3$) δ 0.544 (3H, s, H18), 0.844 (3H, s, H19), 0.863 (3H, d, J = 6.6, H26 or -27), 0.868 (3H, d, J = 6.6, H26 or -27), 0.919 (3H, d, J = 6.5, H21), 3.594 (3H, m, ω1/2 = 26 Hz, H3α), 3.811 (1H, m, ω1/2 = 20 Hz, H6β), 5.182 (1H, d, J = 1.8, H7).

*5α-Cholest-7-en-3β,6β-diol (**24**).* 5α-Cholestan-7-en-6-one-3β-*tert*-butyldimethyl ether (300 mg), prepared from **17** as described for the synthesis of **7**, was dissolved in a mixture of MeOH/THF (2/1, v/v) (35 mL) and was stirred with an excess of sodium borohydride ($NaBH_4$) for 20 h at 4 °C under argon. After usual workup, an aliquot of the residue (40 mg) was treated with tetrabutylammonium fluoride adsorbed on SiO_2, for 24 h at 20 °C with stirring and under argon in THF (4 mL). Usual workup and recrystallization from MeOH afforded pure **24** (16 mg): mp 207−209 °C [Harvey and Bloch (*23*) quote 207−209 °C]; MS (EI) *m*/*e* (relative intensity) M^+ = 402(100), 384(46), 369(22), 366(9), 351(48), 271(54), 253(37); ^{1}H NMR (400 MHz, $CDCl_3$) δ 0.548 (3H, s, H18), 0.864 (3H, d, J = 6.6, H26 or -27), 0.869 (3H, d, J = 6.6, H26 or -27), 0.926 (3H, d, J = 6.5, H21), 0.983 (3H, s, H19), 3.688 (1H, m, ω1/2 = 30 Hz, H3α), 3.914 (1H, bs, ω1/2 = 14 Hz, H6α), 5.448 (1H, ddd, J = 5.4, 2.7, 2.7, H7).

Enzyme Sources and Microsome Preparations. Maize (variety LG11) seedlings were allowed to germinate in moist vermiculite for 60 h at 25 °C. The seedlings were harvested, and the embryos were separated from the caryopses. Microsomes (pH 7.5) were prepared from the seedlings as described previously (*24*).

The strains of *Saccharomyces cerevisiae* which contained the functionally expressed *Arabidopsis thaliana* wild-type and mutated Δ^7-sterol-C5(6)-desaturases were obtained as previously described (*15*). Microsomes (pH 7.5) from these different strains were prepared as described previously (*15*).

Δ^7-Sterol-C5(6)-desaturase Assay. The yeast microsomes (0.4 mL, 1 mg of protein, pH 7.5) were incubated in the presence of deuterated or undeuterated 5α-cholest-7-en-3β-ol **1**, **4**, **21**, or **22** (20−200 μM) emulsified in Tween 80 (final concentration 1.5 g/L) and NADH (500 μM). The incubation was done aerobically at 30 °C with gentle stirring for 60−90 min as described before (*15*). The enzymatic rate was linear during this period. Maize microsomes (0.5 mL, 2 mg of protein, pH 7.5) were incubated in the presence of **1**, **4**, **21**, or **22** (20−200 μM) emulsified in Tween 80 (final concentration 1.5 g/L) and NADH (200 μM), NAD^+ (200 μM) as described before (*3*). Fenpropimorph (**25**) (10 μM) was added to maize microsomes to inhibit sterol-Δ^7-reductase present in this organism (*25*) and possible subsequent metabolism of the $\Delta^{5,7}$-diene produced. Incubations were continued aerobically at 30 °C with gentle stirring for 60−90 min. During this period, the enzymatic rate was linear. Computer-assisted linear regression analysis gave correlation coefficients greater than 0.89 (n = 6−7). In both cases, the reaction was stopped by the addition of 0.5 mL of 6% KOH/EtOH. A definite amount of ergosta-5,7,9,22-tetraen-3β-ol (**3**) was added (5 μg for 0.4 mL incubation) as an internal standard, and the sterols were extracted 3 times with a total volume of 15 mL of *n*-hexane. The extracts were evaporated under argon at 25 °C. The resulting residue was suspended in 50 μL of absolute ethanol, and an aliquot (25 μL) was immediately injected and analyzed by HPLC as described above. The cholesta-5,7-dien-3β-ol (**2**) produced was detected by recording the absorbance of the conjugated double bonds at 281.5 nm and was readily separated from the bulk of endogenous ergosterol. The amount of product formed was calculated by comparison of the integrated peak areas of the known amount of added standard (**2**) and of the $\Delta^{5,7}$-product formed, and corrected from the absorbance coefficient (ϵ) ratio at 281.5 nm between the $\Delta^{5,7}$-sterol produced (**2**) and the standard (**3**) [$\epsilon^{(2)}_{281.5}/\epsilon^{(3)}_{281.5}$ = 2.3], measured under the conditions of the assay. Under these conditions, the estimated limit of detection of the Δ^7-sterol-C5(6)-desaturase activity was 0.02 nmol × h^{-1} × mg^{-1}. The cholesta-5,7-dien-3β-ol produced and the residual substrates **1**, **4**, **21**, and **22** were

collected and further identified by GC and GC-MS (*26*) and allowed us to determine the deuterium labeling, if any, to be quantified. Maximum velocity *V* and *V*/*K* values were determined by fitting the data to the Michaelis−Menten equation using the nonlinear regression program DNRPEASY derived by Duggleby and Leonard from DNRP53 (*27*).

The primary deuterium kinetic isotope effects were defined as $^{D}V = {}^{H}V_{max}/{}^{D}V_{max}$ and $^{D}(V/K) = {}^{H}(V_{max}/K_m)/{}^{D}(V_{max}/K_m)$ according to the conventions of Northrop (*28*, *29*).

Protein Determination. Total membrane protein was determined as described by Bradford (*30*), with bovine albumin as a standard (fraction V, Sigma).

RESULTS AND DISCUSSION

*Synthesis of Deuterium-Labeled 5α-Cholest-7-en-3β-ol Analogues (**4**, **21**, and **22**).* The 6α-deuterated substrate analogue (**4**) was prepared according to an adaptation of the general strategy for the synthesis of 6α-tritiated-5α-cholest-7-en-3*β*-ol (*17*) and is outlined in Scheme 1. In our case, the intermediate 5α-cholest-6-one-3*β*-OBTDMS ether (**7**) was synthesized by regio- and stereoselective hydroboration of the corresponding 5-en derivative (**5**) followed by pyridium dichromate oxidation to produce **7**. The ^{1}H NMR spectrum of the hydroxy derivative (**6**) was in full agreement with that described for the corresponding 3*β*-(2-tetrahydropyranyloxy)-5α-cholestan-6α-ol (*31*); particularly $\delta = 0.806$ (CH-19) attested to an A/B trans ring junction (H-5α). The deuterium atom at C6 was introduced by stereoselective reduction of the α-bromo ketone (**8**) followed by dehydrobromination to yield olefin (**11**) deuterated at C6. The subsequent 6α,7α-epoxide (**13**) was obtained in adequate yield and purity. The *β*-equatorial stereochemistry of the single epoxide proton at C7 was determined from its ^{1}H NMR spectrum since this proton appeared as a doublet with a small 1,2 equatorial−axial coupling constant ($J = 2.3$ Hz). Subsequently, the absence of a large 1,2 axial−axial coupling constant in the signal of the proton at C7 of diol **14** was in accord with the assigned 7α-axial stereochemistry for the hydroxyl at C7 of this derivative which was converted by conventional procedures to the 6α-deuterio-5α-cholest-7-en-3*β*-ol (**4**).

The synthesis of the 5α,6α-dideuterio analogue (**22**) was achieved by diimide reduction of cholesta-5,7-dien-3*β*-ol (*22*) which proceeds by cis-addition of hydrogen (*32*). The ^{1}H NMR spectra of **4** and **22** were in total agreement with that of an authentic sample of 5α-cholest-7-en-3*β*-ol, attesting to the trans A/B ring junction, i.e., 5α-H for **4** and 5α-^{2}H for **22**. The presence of only a small 1,2 coupling constant ($J = 1.9$ Hz) in the signal of the proton at C7 for both **4** and **22** while an additional larger coupling constant ($J = 5$ Hz) was observed for authentic 5α-cholest-7-en-3*β*-ol and the synthetic [5α-^{2}H]-cholest-7-en-3*β*-ol (**21**) attested to an axial 6*β* stereochemistry for the residual proton at C6 of **4** and **22**. Finally, the [5α-deuterio] analogue (**21**) was synthesized as depicted in Scheme 2. The critical [5α-^{2}H]-6α-hydroxy intermediate (**18**) was obtained by the same procedure as that used for the synthesis of **6**. Reductive deoxygenation of **18** using the *N*,*N*,*N*′,*N*′-tetramethylphosphorodiamidate group (*33*) and deprotection of the 3*β*-hydroxyl function afforded the [5α-^{2}H] analogue (**21**). The NMR and mass spectral data indicated that all three [5α]-, [6α]-, and [5α, 6α]-deuterated analogues (**4**, **21**, and **22**) were more than 98% deuterated at each position.

Stereospecificity of the Δ^{7}-Sterol-C5(6)-desaturase Reaction. In an effort to shed more light on the detailed mechanism of Δ^{7}-sterol-C5(6)-desaturase and as a prerequisite for studying DKIE, we first examined the stereospecificity of the hydrogen removal at carbon 6 of 5α-cholest-7-en-3*β*-ol by the 5-DES. Thus, [6α-^{2}H]-5α-cholest-7-en-3*β*-ol (**4**) and [5α-^{2}H, 6α-^{2}H]-5α-cholest-7-en-3*β*-ol (**22**) were incubated with microsomal preparations of *Zea mays* and recombinant *Arabidopsis thaliana* wild-type 5-DESs under the standard assay conditions. These incubations allowed production of a Δ^{5,7}-sterol metabolite which was analyzed and purified by HPLC analysis monitored at 281.5 nm. With all substrates, this metabolite was unequivocally identified as cholesta-5,7-dien-3*β*-ol (**2**) by UV analysis, with coincidental retention times in GC and HPLC and an electron impact spectrum identical to that of an authentic standard. For the three substrates (**4**, **21**, and **22**) and both 5-DESs, the recovered **2** from the HPLC purification had lost more than 99% of the deuterium label at C6 and (or) C5 since no deuterium appeared in the MS of the cholesta-5,7-dien-3*β*-ol produced (data not shown). Moreover, MS analysis of the remaining deuterated substrates indicated that no label was lost during the experimental procedure. The results indicate that the equatorial C6α-hydrogen atom has been specifically removed together with the 5α-hydrogen, attesting to a stereospecific syn 5,6-desaturation during the catalysis by both plant 5-DESs. It was previously reported that the conversion of chemically synthesized [4-^{14}C, 6α-^{3}H]-5α-cholest-7-en-3*β*-ol to cholesterol by a rat liver homogenate preparation proceeded with 94% loss of the labeled hydrogen (*17*). In another study, retention of over 95% of the labeled hydrogen in [4-^{14}C, 6*β*-^{3}H]-cholest-7-en-3*β*-ol upon enzymatic conversion to cholesta-5,7-dien-3*β*-ol by a rat liver homogenate was described (*22*). Our data directly confirm and greatly extend these early observations obtained with the mammalian 5-DES and precursors partially labeled at C5 or C6.

Although the stereochemistry of dehydrogenation reactions has been thoroughly studied in only few cases, the syn dehydrogenation stereochemistry has also been shown to be a feature of another O_2- and NADPH-dependent desaturase, that is, the *Corynebacterium diphteriae* stearyl-C9(10)-desaturase (*34*), and in the desaturation of long-chain fatty acids in *Chlorella vulgaris* (*35*). In contrast, anti-dehydrogenation stereochemistry was found in the case of olefin-forming flavoenzymes such as succinate dehydrogenase (*36*), acyl-CoA dehydrogenases (*37*), or dihydroorotate oxidase (*38*).

Substrate Deuterium Kinetic Isotope Effects on the Reaction Catalyzed by Wild-Type Zea mays and Arabidopsis thaliana Δ^{7}-Sterol-C5(6)-desaturases. The knowledge of the stereochemical course of the 5-DESs and the availability of carbon-deuterated substrate analogues of high isotopic and chiral purity allowed us to determine the intermolecular primary deuterium kinetic isotope effects (DKIEs) for the removal of the 5α- and 6α-hydrogens. The DKIEs determined with 5α-cholest-7-en-3*β*-ol species **4**, **21**, and **22** with the wild-type *Zea mays* and *Arabidopsis thaliana* 5-DES are documented in Table 1 and Figure 3. Similar primary *V* and

Table 1: Observed Deuterium Kinetic Isotope Effects on Δ^7-Sterol-C5(6)-desaturases

substitutions	D_5H_6 vs H_5H_6	H_5D_6 vs H_5H_6	D_5D_6 vs H_5H_6	D_5D_6 vs D_5H_6	D_5D_6 vs H_5D_6
Zea mays wild type					
^{D}V	0.99[a] ± 0.04	2.59 ± 0.35	2.43 ± 0.25	2.49 ± 0.36	0.95 ± 0.05
$^{D}(V/K)$	0.91[a] ± 0.08	2.41 ± 0.07	2.30 ± 0.10	2.53 ± 0.24	0.96 ± 0.06
A. thaliana wild type					
^{D}V	0.93 ± 0.06	2.25 ± 0.28	2.26 ± 0.07	2.44 ± 0.02	1.02 ± 0.09
$^{D}(V/K)$	0.96 ± 0.04	2.28 ± 0.22	2.12 ± 0.32	2.20 ± 0.28	0.93 ± 0.06
A. thaliana T114S					
^{D}V	0.96 ± 0.05	1.60 ± 0.37	1.80 ± 0.41	1.58 ± 0.06	1.09 ± 0.20
$^{D}(V/K)$	0.96 ± 0.04	1.69 ± 0.13	1.59 ± 0.20	1.68 ± 0.22	0.97 ± 0.02
A. thaliana T114I					
^{D}V	1.10 ± 0.08	3.80 ± 0.30	3.21 ± 0.12	2.94 ± 0.30	nd[b]
$^{D}(V/K)$	1.23 ± 0.29	3.76 ± 0.36	3.35 ± 1.5	2.56 ± 0.60	nd

[a] Velocities and V/K values were determined by fitting the data to the Michaelis−Menten equation using the nonlinear regression program DNRPEASY derived by Duggleby and Leonard from DNRP53 (*27*). The means ± SD were calculated from the values resulting from two or three separate experiments. The primary deuterium kinetic isotope effects were defined as $^{D}V = {}^{H}V_{max}/{}^{D}V_{max}$ and $^{D}(V/K) = {}^{H}(V_{max}/K_m)/{}^{D}(V_{max}/K_m)$ according to the conventions of Northrop (*28, 29*). [b] nd: not determined.

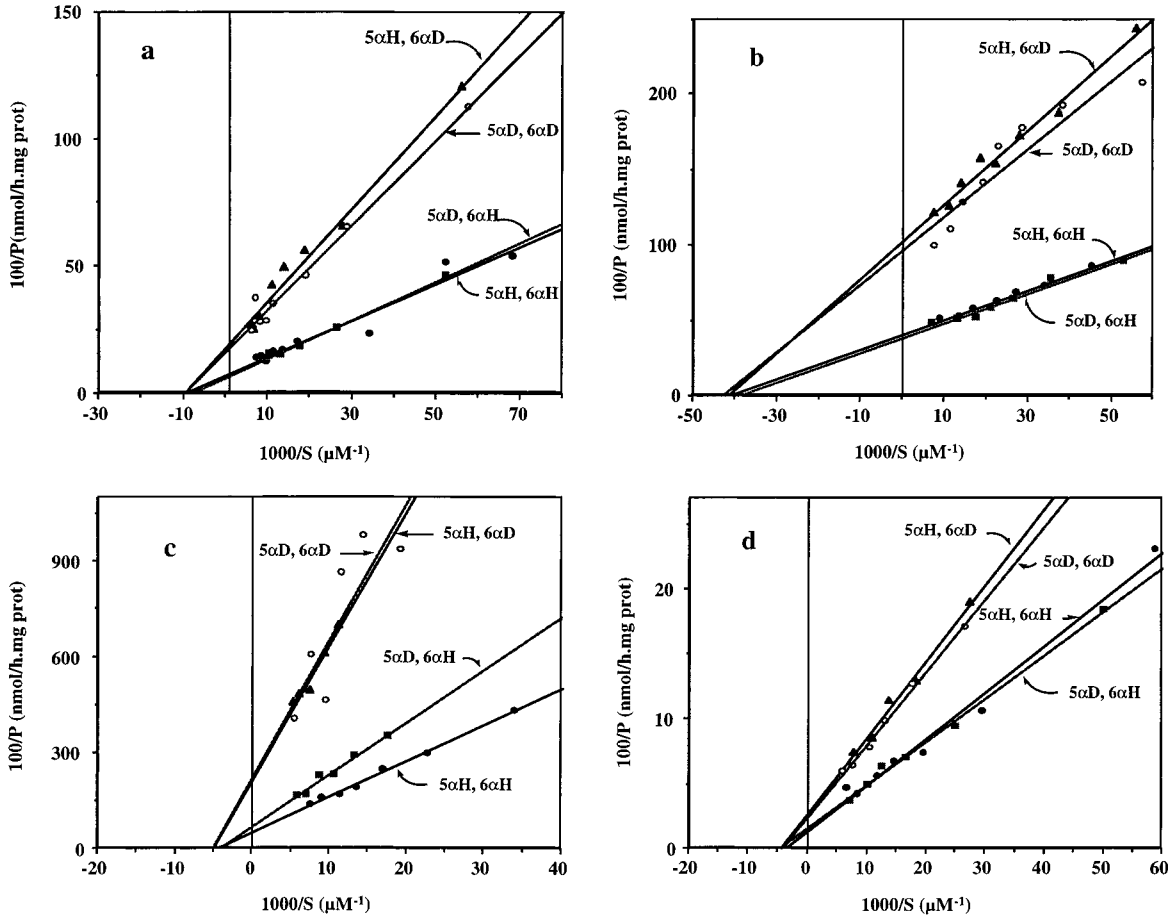

FIGURE 3: Examples of double-reciprocal plots of Δ^7-sterol-C5(6)-desaturase activity with various deuterium-labeled cholest-7-en-3β-ol. Assays were conducted as described under Materials and Methods. Straight lines were fitted by using a computer-assisted least-squares method (Cricket Graph). (a) *Zea mays* C5(6)-desaturase; (b) wild-type *A. thaliana* C5(6)-desaturase; (c) *A. thaliana* mutant T114I C5(6)-desaturase; (d) *A. thaliana* mutant T114S C5(6)-desaturase.

V/K deuterium isotope effects were determined for the carbon−hydrogen bond cleavage at C6: $^{D6}V = 2.6 \pm 0.3$, $^{D6}(V/K) = 2.4 \pm 0.1$ and $^{D6}V = 2.3 \pm 0.35$, $^{D6}(V/K) = 2.3 \pm 0.2$ for the *Zea mays* and *Arabidopsis thaliana* 5-DES, respectively. In contrast, negligible isotope effects whose extents fall in the range of the experimental lack of precision, $^{D5}V = 0.99 \pm 0.04$, $^{D5}(V/K) = 0.91 \pm 0.08$ and $^{D5}V = 0.93 \pm 0.06$, $^{D5}(V/K) = 0.96 \pm 0.04$, were respectively observed for the C5−H bond breaking. With compound **22**, which incorporates the labels of both **4** and **21**, qualitatively similar values to those obtained with the C6-monodeuterated substrate **4** were observed: $^{D5,6}V = 2.4 \pm 0.2$, $^{D5,6}(V/K) = 2.3 \pm 0.1$ and $^{D5,6}V = 2.3 \pm 0.1$, $^{D5,6}(V/K) = 2.1 \pm 0.3$, respectively. For the three substrates **4**, **21**, and **22**, the data obtained for the V/K isotope effects are closed to the respective V_{max} effects. However, the precision on the KIEs is not sufficient to conclude definitely that the V and V/K effects are the same. Nevertheless, $^{D}V > 1.0$ suggests that product dissociation from the enzyme is not rate-limiting, and $^{D}(V/K) > 1.0$ is consistent with a nonsticky substrate (*39*).

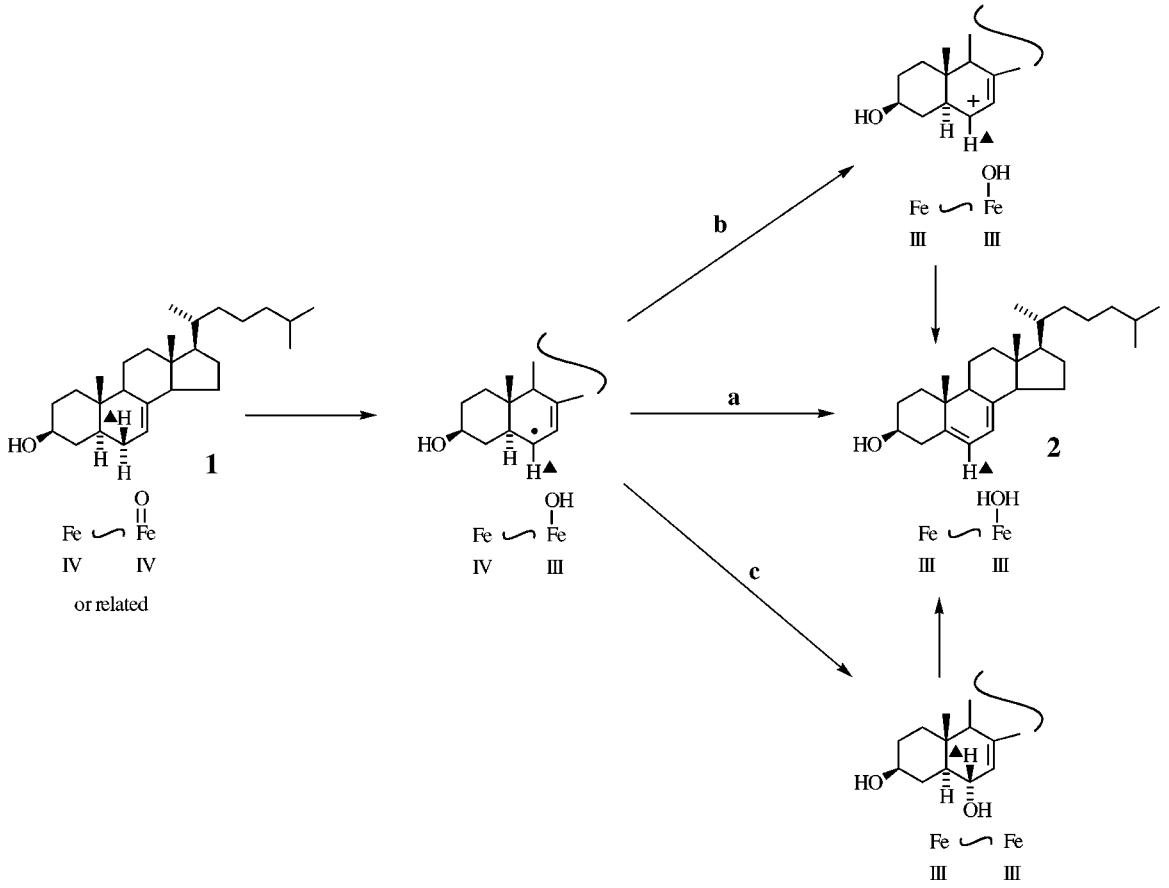

FIGURE 4: Possible mechanistic scheme for the desaturation of cholest-7-en-3β-ol.

To our knowledge, our data represent together with the early work of Enoch et al. (*40*), who measured a substantial intermolecular deuterium KIE using a purified rat liver desaturase system, the only direct kinetic intermolecular primary deuterium isotope effect determination in a desaturation process carried out by a membrane-bound non-heme iron desaturase. The obtained results indicate that cleavage of the substrate C6α−H bond is a partially rate-determining step for desaturation. Cleavage of the C5−H bond for the latter has a negligible isotope effect, indicating that the desaturation involves asynchronous scission of the two C−H bonds.

The magnitude of the primary DKIEs observed at C6 is significantly less than the theoretical value of 7−8 (*28*), as expected for a "rate-determining" C−H bond cleavage in an enzyme-catalyzed reaction. The phenomenon known as "masking" is encountered frequently in isotope effect experiments which, like our study, employ an intermolecular design. For example, a substantial intramolecular primary DKIE at C4 (5.58) and a significantly lower value at C5 (1.62) were measured for the cytochrome P-450 mediated 4,5-dehydrogenation of valproic acid (*41*), while the corresponding values for the intermolecular DKIEs (2.2 and 0.8) were much smaller. Similarly, intermolecular DKIEs on the catalytic constants of 2.8 and 1.3 for hydrogen abstraction in cytochrome P-450 dependent [1-$^2H_2$]-benzyl alcohol oxidation (*42*) demonstrated that DKIEs for P-450-catalyzed hydrocarbon hydroxylations calculated on V_{max} are generally small (*43*). Observed isotope effects may be significantly suppressed by the relative kinetic relationship of the isotopically sensitive step to other steps in the overall turnover cycle, and the observed DKIE represents the lower limits of the intrinsic isotope effects on the chemical step of interest (*29*). The determination of a small ^DV isotope effect thus may be indicative of a rate-limiting step distinct from (and probably occurring after) the observed isotopically sensitive step (*29*). However, in nonenzymatic reactions involving rate-limiting hydrogen atom abstraction, small kinetic isotope effects have also been attributed to asymmetric or nonlinear bond streching in the transition state (*44*−*47*).

The existence of a kinetic isotope effect for the abstraction of *one* hydrogen appears to be present in several non-heme iron fatty-acid desaturases such as the Δ^9-stearoyl-CoA desaturase from different organisms (*34*, *48*), the *A. thaliana* Δ^{12}-oleyl-CoA desaturase (*49*), a Δ^6-desaturase (*50*), and the Δ^{11}-myristoyl-CoA desaturase (*51*), as well as in the cytochrome P-450-mediated desaturation of valproic acid (*41*). In contrast, dihydroorotate oxidase, a desaturase mediated by a flavoenzyme, has been found to involve kinetically significant transition states for both C−H bond breaking step at C5 and C4 of dihydroorotate (*38*). Taken together, these data suggest that the above-mentioned O_2- and NAD(P)H-dependent desaturases would follow a similar reaction mechanism. This mechanism could be linked to that depicted for hydroxylation of nonactivated carbon by either cytochrome P-450-dependent (*43*, *52*) or non-heme iron hydroxylases (*53*, *54*), in accordance with the mounting evidence that desaturases and hydroxylases are structurally related proteins (*11*, *55*).

Possible mechanisms for desaturation at C5(6) of Δ^7-sterol, adapted from that previously proposed for oleate Δ^{12}-desaturase (*49*), are shown in Figure 4. Initial abstraction of

the 6α-hydrogen atom at C6 to form a substrate radical might occur similarly to that proposed for hydroxylase reactions, by a hypervalent iron−oxo species. This species would collapse to olefin via different pathways (Figure 4), including a possible alcohol intermediate pathway (pathway c) and an electron transfer to the ferryl species from the carbon radical intermediate, generating a carbocationic intermediate (pathway b), followed by transfer of a proton from the substrate to the iron-bound oxygen, or simple disproportionation (pathway a). Previous in vitro studies have suggested that the conversion of cholest-7-en-3*β*-ol (**1**) to cholesta-5,7-dien-3*β*-ol (**2**) does not appear to involve a 6*β*-hydroxy, a 6α-hydroxy, or a 6-keto intermediate, while the conversion of cholest-7-en-3*β*,6*β*-diol by a rat liver homogenate to cholesterol was described under aerobic conditions (*56*). In the present work, incubation of synthetic 5α-cholest-7-en-3*β*,6α-diol (**23**) and 5α-cholest-7-en-3*β*,6*β*-diol (**24**) in the standard conditions with a microsomal preparation from wild-type recombinant *Arabidopsis thaliana* desaturase did not produce any detectable cholesta-5,7-dien-3*β*-ol. Moreover, we could not detect within the experimental limit of detection any formation of **23** or **24** during HPLC analysis (monitored at 210 nm) for standard incubations of **2** with the same microsomal preparation. These results are consistent with the conclusion that alcohols **23** and **24** are probably not discrete intermediates of the C5(6) desaturation process. Thus, we consider pathway c to be an unlikely route to the 5,7-diene product (**2**).

We next examined pathway b by challenging the 5-DES with the 6-aza-B-homosteroid (**26**), an analogue of a carbocationic intermediate at C5−C7 (*57*). We could not observe any significant in vitro inhibition of the 5-DES by this derivative, which is a powerful inhibitor of the $\Delta^{5,7}$-sterol-Δ^7-reductase involving a C5−C7 carbocationic intermediate (*57*). Consistent with these data, in vivo treatment of bramble cell suspension cultures by this compound did not lead to any accumulation of Δ^7-sterols (*57*). These data would argue against the passage through the putative carbocationic intermediate at C6 in pathway b.

Thus, our cumulative data are most consistent with the proposed pathway a involving a stepwise removal of the C-6α hydrogen by an iron-bound oxygen to generate a carbon-centered radical at C6 which furnishes the desaturated product by a disproportionation reaction. Furthermore, we recently showed (*15*) that the eight histidines from three histidine-rich motifs from the 5-DES were essential for the catalytic activity, suggesting that they could provide the ligands for a presumed catalytic Fe center, as previously proposed for a number of integral membrane enzymes catalyzing desaturations and hydroxylations (*11, 13*).

Our results are also in line with the growing amount of evidence suggesting a close similarity between the mechanisms of desaturation and hydroxylation reactions of unactivated hydrocarbons. Other hydroxylation and desaturation processes for which this relationship have been suggested include conventional cytochrome P-450 mediated dehydrogenations, in which the crucial carbon radical is produced through cleavage of a C−H bond to furnish the desaturated product by a disproportionation reaction (*41, 58*). In the case of the 5-DES, what governs the orientation of the reaction pathway to desaturation at C5−6 versus possible hydroxylation at C6 is not currently understood and presumably reflects the precise organization within the Michaelis complex to produce a preferential loss of the C5 hydrogen to form an olefin instead of C−O bond formation to form an alcohol at C6. It would be interesting to disturb this organization through the use of alternate substrates or mutagenized enzyme to direct the reaction toward hydroxylation instead of olefin production.

To conclude this section, the observed primary DKIEs indicate considerable C6α−H bond stretching in a partially rate-controlling transition state for desaturation of **1**. These DKIEs and other data mentioned herein are consistent with a mechanistic scheme involving a two-step reaction in which initial hydrogen abstraction at C6 is slow relative to the second step and presumably leads to the formation of a carbon-centered radical at C6 as a discrete intermediate. They are not consistent with a concerted C5(6)-desaturase mechanism, a possibility which has been raised previously (*59*). Thus, our results provide evidence for a reaction pathway similar to that previously proposed in the case of the membrane-bound and non-heme diiron cluster containing steroyl CoA-Δ^9-desaturase (*48*).

Substrate Deuterium Kinetic Isotope Effects on the Reaction Catalyzed by Arabidopsis thaliana C5(6)-Desaturase Mutated at Position 114. Cloning and expression of the gene for *A. thaliana* 5-DES in *S. cerevisiae* allowed studying by mutational analysis, coupled with kinetic studies, the role of highly conserved residues in the reaction catalyzed by the 5-DES (*15*). Recently, an *A. thaliana* recessive mutant (*ste1*) accumulating Δ^7-sterols at the expense of Δ^5-sterols was described (*60*). When compared to the wild-type 5-DES, the *ste1* 5-DES possesses a single amino acid substitution: threonine 114 in the wild type is changed to isoleucine in *ste1* (*61*). We recently showed that the T114I mutation was responsible for the low activity of the *ste1* 5-DES but that threonine 114 was not essential to maintaining the 5-DES activity (*15*). However *V*/*K* values for mutants T114I and T114S were respectively 10-fold lower and 4-fold higher than that of the native 5-DES. We used the methodology described in this paper with these two mutants at position 114 to obtain further insight in the role of threonine 114 in catalysis by the 5-DES from *A. thaliana*.

We first checked the stereochemistry of both mutant desaturases. In both cases we also observed complete loss of the deuterium label at the C6 position while no loss of label from the remaining substrates was detected. Thus, the mutant desaturases were found to show the same stereochemical integrity as the wild-type enzyme. The two mutants produced cholesta-5,7-dien-3*β*-ol **2**, and we could not detect any formation of diols **23** or **24** during monitoring of the enzymatic assay at 210 nm (within the experimental limit of detection). Next, the DKIEs on V_{max} and *V*/*K* were determined (Table 1 and Figure 3). Primary DKIEs $^{D6}V = 3.8 \pm 0.3$, $^{D6}V/K = 3.8 \pm 0.4$ and $^{D6}V = 1.6 \pm 0.4$, $^{D6}V/K = 1.7 \pm 0.1$ were determined for mutants T114I and T114S, respectively. A negligible or minor DKIE was observed for removal of the C5 hydrogen ($^{D5}V = 0.96 \pm 0.05$, $^{D5}V/K = 0.96 \pm 0.04$) with mutant T114S ($^{D5}V = 1.1 \pm 0.1$, $^{D5}V/K = 1.2 \pm 0.3$) or with mutant T114I. Qualitatively similar values to those obtained with the C6-monodeuterated substrate **4** were obtained with compound **22** which incorporates the labels of both **4** and **21** (Table 1). However, for mutant T114I, it was not possible to measure with sufficient

precision the kinetic parameters allowing calculation of the DKIEs at C5 in the presence of label at C6 (D5D6 vs H5D6), because of the reduced catalytic rate of this mutant in addition to its increased DKIE at C6.

Taken together, the data first indicate a primary DKIE pattern for the T114 mutant desaturases that is qualitatively similar to that observed for the wild-type desaturase, suggesting a similar reaction pathway for these isoforms. In other words, cleavage of C5α−H and C6α−H does not occur in a single transition state. The DKIEs for *V* and *V*/*K* with 6α-deuteriocholest-7-en-3*β*-ol (**4**) for mutant T114I, whose V_m and *V*/*K* are respectively 70% and 10% those of the wild-type 5-DES (*15*), were both substantially increased to 3.8. Conversely, they were decreased to 1.7 and 1.6, respectively, for mutant T114S which displays a 28-fold higher V_m value and a 4-fold higher *V*/*K* value than the wild-type 5-DES. These data indicate that a hydroxyl-containing side chain at position 114 substantially increases the catalytic rate of the 5-DES and makes the deuterium-sensitive step less rate-limiting. There is no evidence that the intrinsic isotope effect is changed in the mutants. Rather it is likely that the chemistry is slower in the T114I mutant, decreasing the commitment and resulting in a more fully expressed KIE, closer to the intrinsic value (*29*). Conversely, in the case of mutant T114S, the chemistry is faster, but subsequent steps, as product release, change less, so that the observed KIEs are smaller.

How Thr114 exerts its effects on catalysis and, specifically, its role in the abstraction of C6α−H are currently unknown. Although mutation at position 114 led to the same stereochemical outcome, changing the nature of the side chain at position 114 could lead to alterations in the orientation of substrate binding during catalysis and specifically could alter the distance and relative orientation of the C6α hydrogen atom to the putative iron−oxo species, thus affecting the rate of cleavage of the C6α−H bond. Recent studies with the methane-monooxygenase hydroxylase, exemplifying the class of soluble non-heme iron monooxygenases possessing a consensus motif consisting of carboxylates and histidines that are thought to act to coordinate an active iron cluster, have revealed that protons are required in the O_2 activation steps of this diiron hydroxylase (*62*). As discussed for the P450 family, the H-bonding interactions observed in soluble diiron hydroxylases and desaturases suggest that a Thr residue may have an important role in catalysis, possibly by acting as a proton donor in the O_2 activation step of the reaction cycle (*63*). However, it was recently shown in the case of the diiron enzyme toluene 4-monooxygenase that the corresponding threonine residue (Thr201) is not required for catalysis, making the reason for conservation of this amino acid in this family of enzymes unclear (*64*). A hydroxyl function is conserved at position 114 in the ERG3 family (*15*). Similarly, it is not essential for the activity but leads to the highest catalytic rates of the *A. thaliana* 5-DES (*15*). From the data concerning the impact of the mutations at position 114 on the DKIE at C6 and on the overall desaturation process (*15*), we cannot conclude whether abstraction of the C6α-hydrogen is the only sensitive step to mutation at position 114. We cannot exclude the above-mentioned participation of Thr114 in the transmission of protons through a network of H-bonded water molecules and amino acid residues connected to the active site.

In conclusion, the methodology used in this study represents a useful approach for further investigations to elucidate the relative contribution of key residues to the 5-DES reaction process and other membrane-associated non-heme iron desaturases.

ACKNOWLEDGMENT

We are indebted to B. Bastian for typing the manuscript. We thank A. Hoeft for GC-MS analysis and technical assistance. We are grateful to Dr. I. A. Kagan for correcting the English and to J. D. Sauer for recording the NMR spectra.

REFERENCES

1. Benveniste, P. (1986) *Annu. Rev. Plant Physiol. 1986*, 275−308.
2. Benveniste, P., and Rahier, A. (1992) in *Target sites of fungicide action* (Köller, W., Ed.) pp 207−225, CRC Press, Boca Raton.
3. Taton, M., and Rahier, A. (1996) *Arch. Biochem. Biophys. 325*, 279−288.
4. Kawata, S., Trzaskos, J. M., and Gaylor, J. L. (1985) *J. Biol. Chem. 260*, 6609−6617.
5. Osumi, T., Nishimo, T., and Katsuki, H. (1979) *J. Biochem. 85*, 819−826.
6. Reddy, V. V. R., Kupfer, D., and Caspi, E. (1977) *J. Biol. Chem. 252*, 2797−2801.
7. Rahier, A., Smith, M., and Taton, M. (1997) *Biochem. Biophys. Res. Commun. 236*, 434−437.
8. Arthington, B. A., Benett, L. G., Stakud, P. L., Guynn, C. J., Barbuch, R. J., Ulbright, C. E., and Bard, M. (1991) *Gene 102*, 39−44.
9. Gachotte, D., Husselstein, T., Bard, M., Lacroute, F., and Benveniste, P. (1996) *Plant J. 9*, 391−398.
10. Matsushima, M., Inazawa, J., Takahashi, E., Suzumori, K., and Nakamura, Y. (1996) *Cytogenet. Cell Genet. 74*, 252−254.
11. Shanklin, J., Whittle, E., and Fox, B. G. (1994) *Biochemistry 33*, 12787−12794.
12. Avelange-Macherel, M. H., Macherel, D., Wada, H., and Murata, N. (1995) *FEBS Lett. 361*, 111−114.
13. Shanklin, J., Achim, C., Schmidt, H., Fox, B. G., and Münck, E. (1997) *Proc. Natl. Acad. Sci. U.S.A. 94*, 2981−2986.
14. Lee, M., Leuman, M., Banas, A., Bafor, M., Singh, S., Schweizer, M., Nilsson, R., Liljarberg, C., Dahlqvist, A., Gummeson, P.-O., Sjödahl, S., Green, A., and Stymne, S. (1998) *Science 280*, 915−918.
15. Taton, M., Husselstein, T., Benveniste, P., and Rahier, A. (2000) *Biochemistry 39*, 701−711.
16. Shanklin, J., and Cahoon, E. B. (1998) *Annu. Rev. Plant Physiol. Mol. Biol. 49*, 611−641.
17. Akhtar, M., and Marsh, S. (1967) *Biochem. J. 102*, 462−467.
18. Hosoda, H., Fukushima, D. K., and Fishman, J. (1973) *J. Org. Chem. 38*, 4209−4211.
19. Corey, E. J., and Schmidt, G. (1979) *Tetrahedron Lett. 5*, 399−402.
20. Fieser, L. F., and Heymann, H. (1952) *Helv. Chim. Acta 35*, 631−636.
21. Dolle, F., Hetru, C., and Luu, B. (1994) *Tetrahedron 47*, 7059−7066.
22. Paliokas, A. M., and Schroepfer, G. J., Jr (1968) *J. Biol. Chem. 243*, 453−464.
23. Harvey, W. E., and Bloch, K. (1961) *Chem. Ind. 1961*, 595−596.
24. Pascal, S., Taton, M., and Rahier, A. (1993) *J. Biol. Chem. 268*, 11639−11654.
25. Taton, M., and Rahier, A. (1991) *Biochem. Biophys. Res. Commun. 181*, 465−473.
26. Rahier, A., and Benveniste, P. (1989) in *Analysis of sterols and other significant steroids* (Nes, W. D., and Parish, E., Eds.) pp 223−250, Academic Press, New York.

27. Duggleby, R. G. (1984) *Comput. Biol. Med. 14*, 447−455.
28. Northrop, D. B. (1975) *Biochemistry 14*, 2644−2652.
29. Northrop, P. B. (1982) *Methods Enzymol. 87*, 607−625.
30. Bradford, M. (1976) *Anal. Biochem. 72*, 248−254.
31. Arnostova, L. M., Pouzar, V., and Drasar, P. (1992) *Steroids 57*, 233−235.
32. Corey, E. J., Pasto, D. J., and Mock, W. L. (1961) *J. Am. Chem. Soc. 83*, 2957−2958.
33. Ireland, R. E., Muchmore, D. C., and Hengartner, U. (1972) *J. Am. Chem. Soc. 94*, 5098−5100.
34. Schroepfer, G. J., Jr., and Bloch, K. (1965) *J. Biol. Chem. 240*, 54−63.
35. Morris, L. J., Harris, R. V., Kelly, W., and James, A. T. (1968) *Biochem. J. 109*, 673−678.
36. Tchen, T., and Milligan, H. (1960) *J. Am. Chem. Soc. 82*, 4115−4116.
37. Biellmann, J. F., and Hirth, C. G. (1970) *FEBS Lett. 9*, 335−339.
38. Pascal, R. A., Jr., and Walsh, C. T. (1984) *Biochemistry 23*, 2745−2752.
39. Cook, P. F., and Cleland, W. W. (1981) *Biochemistry 20*, 1790−1796.
40. Enoch, H. G., Catala, A., and Strittmatter, P. (1976) *J. Biol. Chem. 251*, 5095−5103.
41. Rettie, A. E., Boberg, M., Rettenmeier, A. W., and Baillie, T. A. (1988) *J. Biol. Chem. 263*, 13733−13738.
42. Vaz, A. D. N., and Coon, M. J. (1994) *Biochemistry 33*, 6442−6449.
43. Ortiz de Montellano, P. R. (1995) in *Cytochrome P-450* (Ortiz de Montellano, P. R., Ed.) pp 245−304, Plenum Publishing Corp., New York.
44. More O'Fenall, R. A. (1970) *J. Chem. Soc., B*, 785−790.
45. Kwart, H., and Latimore, M. C. (1971) *J. Am. Chem. Soc. 93*, 3770−3771.
46. Pryor, W. A., and Kneipp, K. G. (1971) *J. Am. Chem. Soc. 93*, 5584−5586.
47. Bethell, D., Hare, G. J., and Kearney, P. A. (1981) *J. Chem. Soc., Perkin Trans. 2*, 684−691.
48. Buist, P. H., and Beharouzian, B. (1996) *J. Am. Chem. Soc. 118*, 6295−6296.
49. Buist, P. H., and Behrouzian, B. (1998) *J. Am. Chem. Soc. 120*, 871−876.
50. Baenziger, J. E., Smith, I. C. P., and Hill, R. J. (1990) *Chem. Phys. Lipids 54*, 17−23.
51. Pinilla, A., Camps, F., and Fabrias, G. (1999) *Biochemistry 38*, 15272−15277.
52. Newcomb, M., Le Tadic-Biadatti, M. H., Chetney, D. L., Roberts, E. S., and Hollenberg, P. F. (1995) *J. Am. Chem. Soc. 117*, 12085−12091.
53. Feig, A. L., and Lippard, S. J. (1994) *Chem. Rev. 94*, 759−805.
54. Valentine, A. M., Wilkinson, B., Liu, K. E., Komar-Parnicucci, S., Priestley, N. D., Williams, P. G., Morimoto, H., Floss, H. G., and Lippard, S. J. (1997) *J. Am. Chem. Soc. 119*, 1818−1827.
55. Fox, B. G., Shanklin, J., Ai, J., Loehr, T. M., and Sanders-Loehr, J. (1994) *Biochemistry 33*, 12776−12786.
56. Slaytor, M., and Bloch, K. (1965) *J. Biol. Chem. 240*, 4598−4602.
57. Rahier, A., and Taton, M. (1996) *Biochemistry 35*, 7069−7076.
58. Lee-Robichaud, P., Shyadehi, A. Z., Wright, J. N., Akhtar, M. E., and Akhtar, M. (1995) *Biochemistry 34*, 14104−14113.
59. Dewhurst, S. M., and Akhtar, M. (1967) *Biochem. J. 105*, 1187−1193.
60. Gachotte, D., Meens, R., and Benveniste, P. (1995) *Plant J. 8*, 407−416.
61. Husselstein, T., Schaller, H., Gachotte, D., and Benveniste, P. (1999) *Plant Mol. Biol. 39*, 891−906.
62. Lee, S. K., and Lipscomb, J. D. (1999) *Biochemistry 38*, 4423−4432.
63. Fox, B. G., Shanklin, J., Ai J., Loehr, T. M., and Sanders-Loehr, J. (1994) *Biochemistry 33*, 12776−12786.
64. Pikus, J. D., Mitchell, K. H., Studts, J. M., McClay, K., Steffan, R. J., and Fox, B. G. (2000) *Biochemistry 39*, 791−799.

BI001696B